Typeset using LaTeX **preprint** style in AASTeX631
a Draft version April 26, 2024

ASTR 302: R Filter Observations of a Proto-Helium White Dwarf in the EL-CVn Binary WASP0845+53

Nicolas Mazziotti,[1]

(Group Members: Shea DeFour-Remy, Tintin Nguyen, Keita Maekawa, Swapnaneel Dey)

[1] *University of Arizona Department of Astronomy*

ABSTRACT

WASP0845+53 is an EL-CVn type binary consisting of a proto-helium white dwarf orbiting around a A-type dwarf star. Existing observations of this binary have only been conducted in a single bandpass, therefore multi-bandpass observations are needed to further constrain the binary parameters of the system. We observed WASP0845+53 in the R filter with the 61" Kuiper telescope during a primary eclipse using the Mont4k CCD camera. We produced a light curve of this eclipse and found the magnitude increase to be 0.0434 as the secondary star fully eclipses the primary. Combining our light curve results with existing measurements of this system's binary parameters, we determined the orbital period, stellar radii ratio, and luminosity ratio to be $P = 0.855$ days, $R_B/R_A = 0.127$, and $L_B/L_A = 0.2002$. Our results generally agree with the existing constraints on these parameters. We conclude that proto-helium white dwarf likely evolved to its current mass through significant mass transfer to the primary star, though current mass transfer is likely not occurring.

Keywords: binaries — EL-CVn binaries — white dwarfs — stellar astronomy

1. INTRODUCTION

1SWASPJ084558.78+530209.8 (hereafter WASP0845+53) is a proto-helium white dwarf (pre-He-WD) in a EL CVn-type binary, first discovered in Maxted et al. (2014). EL CVn-type binaries consist of a main sequence A-type dwarf star with a smaller, hotter companion star on track to become a helium white dwarf. The light curves of EL CVn-type binaries are characteristic of a total eclipse: a primary eclipse occurs when the companion eclipses the primary star, and a secondary eclipse occurs when the primary star eclipses the secondary star. WASP0845+53 was identified through the Wide Angle Search for Planets (WASP; Pollacco et al. 2006) by Maxted et al. to study eclipsing binary systems similar to WASP 0247–25, which was discussed at length in Maxted et al. (2011). Bright binary systems like WASP 0247–25 offer favorable conditions to better understand low-mass white dwarfs when they are in the pre-He-WD stage.

The WASP data used in Maxted et al. has only a single bandpass, roughly spanning the I filter. In this filter, Maxted et al. determined the mass of the primary star to be $1.45M_\odot$ with an effective temperature of 8000 K, while the pre-He-WD was found to have a mass of $0.19M_\odot$ with an effective

temperature of 15000 K. Multi-bandpass observations of WASP0845+53 are necessary to further constrain the binary parameters at higher precision, particularly the temperature of each star in different wavelengths. In this work, we present observations of WASP0845+53 in the R filter as part of an ongoing effort to obtain high S/R, UBVR light curves for this system.

2. OBSERVATIONS

A primary eclipse of WASP0845+53 was observed using the Mont4k CCD camera[1] on the 61" Kuiper telescope on Mt. Bigelow, Arizona. Due to inclement weather on scheduled observing nights, we were unable to obtain sufficient data for a primary eclipse ourselves and instead have opted to use existing data of a primary eclipse observed on February 26, 2023, in the R filter. 482 exposures were taken over the span of roughly 5.5 hours with 30 second exposure times each. A 2x2 pixel summing was applied across the CCD.

3. DATA ANALYSIS

3.1. *Data Processing*

Observations were processed with AstroImageJ (AIJ; Collins et al. 2017), a graphical user interface intended for reducing and calibrating astronomical image data. The CCD Data Processor tool on AIJ was used to bias correct and flat field all 482 images. Averaging across the two CCD amplifiers, each exposure had a gain of 3.1595 e^-/DN, a dark current of 0.0 e^-/pixel/hour, and a readout noise of 6.54 e^-. Airmass during observations ranged from approximately 2.33 to 726.03.

3.2. *Differential Photometry*

After processing the data, AIJ was used to perform differential photometry on the field. A total of six reference stars were chosen close to the target, shown in Figure 1. Apertures for the object, inner sky annulus, and outer sky annulus were initially set 10, 15, and 20 pixels, respectively. After running multi-aperture photometry with AIJ, these apertures were automatically adjusted to 17, 29, and 44 pixels. Relative fluxes were then calculated by AIJ and exported to a light curve. Figure 2 displays the light curve of the primary eclipse before removing systematic offset, while Figure 3 displays the light curve after fitting a fourth-degree polynomial to each phase of the transit in a piecewise fashion. The flux drop during the eclipse was measured to be 0.0093, resulting in an increase of apparent magnitude around 0.0434. The average signal-to-noise ratio of our target was 1238.76. Table 1 contains sample data of ten exposures of the target (labeled T1) after processing the data and performing differential photometry.

4. SCIENTIFIC ANALYSIS

Figure 4 contains a schematic of the primary eclipse as the pre-He-WD, labeled star B, transits across the primary star, labeled star A. To perform our analysis, we assume the orbital dynamics of this system can be approximated by a circular orbit. The orbital velocity of the secondary star will then remain constant over time, and will be approximately equal to the observed velocity as the secondary star eclipses the primary. During ingress, the secondary will travel a distance equal to its diameter in some time τ. The time it takes for the secondary to begin egress after ingress is defined as T. During the time $\tau + T$, the secondary subsequently traverses the entire diameter of

[1] http://james.as.arizona.edu/ psmith/61inch/CCD/basicinfo.html

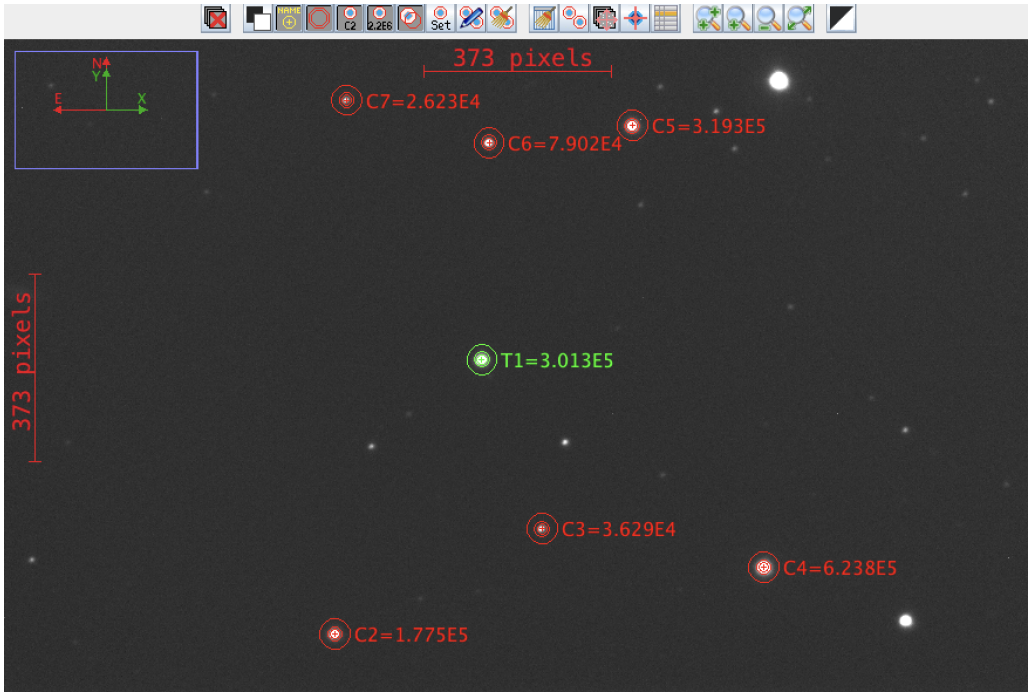

Figure 1. Screenshot of multi-aperture photometry tool in AstroImageJ. WASP0845+53 (T1) is labeled in green while all reference stars (C2-7) are labeled in red.

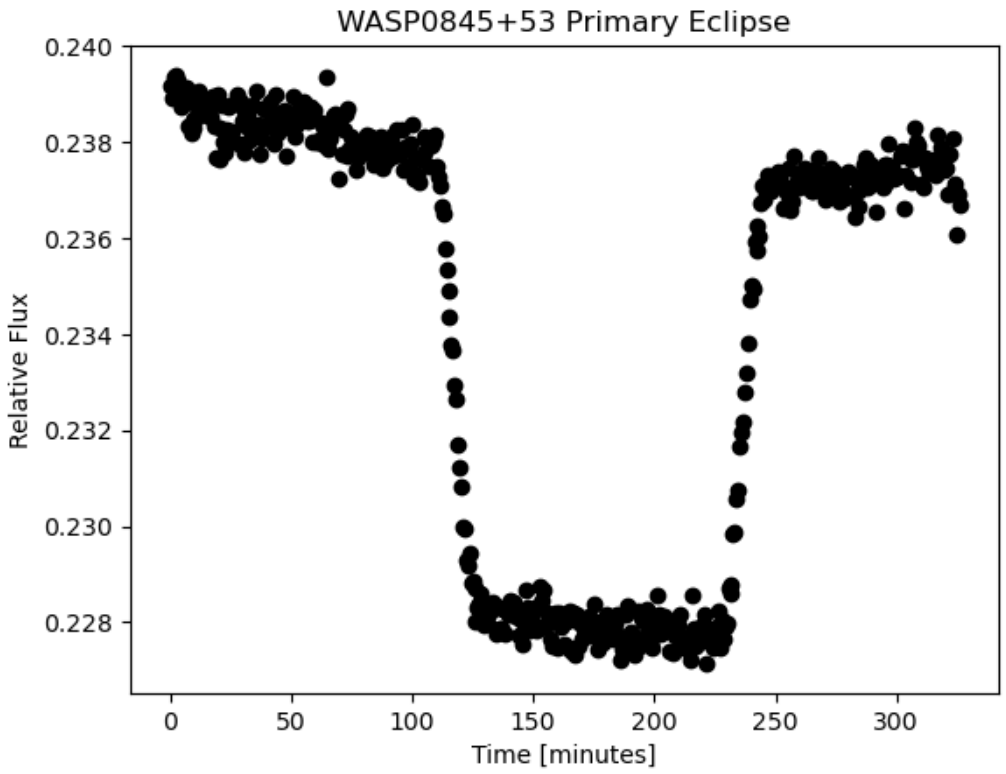

Figure 2. Light curve in R filter of primary eclipse before removal of systematic offset.

Table 1. Sample data of 10 exposures after processing and differential photometry with AIJ

Label	HJD_UTC	rel_flux_T1	rel_flux_err_T1	rel_flux_SNR_T1
wasp0845.0146_out.fits	2460002.718140290	0.2375155210475770	0.0001880947157938	1262.7442511889300
wasp0845.0147_out.fits	2460002.718609720	0.2379674330087230	0.0001887400763794	1260.820900222640
wasp0845.0148_out.fits	2460002.7190781300	0.2383870199744080	0.0001889998568619	1261.3079392361900
wasp0845.0149_out.fits	2460002.71954908	0.2372540361336470	0.0001877721614982	1263.5208235377800
wasp0845.0150_out.fits	2460002.720019580	0.2376871749022040	0.0001878118058011	1265.5603511627300
wasp0845.0151_out.fits	2460002.7204895100	0.2373087313873170	0.0001875289696238	1265.4510493142300
wasp0845.0152_out.fits	2460002.720959760	0.2371687224440010	0.0001882694718458	1259.7301098199500
wasp0845.0153_out.fits	2460002.7214293400	0.2376469617893410	0.0001878501525481	1265.0879361331200
wasp0845.0154_out.fits	2460002.7219000600	0.2376476498953990	0.0001880650260236	1263.6461702645000
wasp0845.0155_out.fits	2460002.722369470	0.2377930112381310	0.0001885906641864	1260.8949242742400

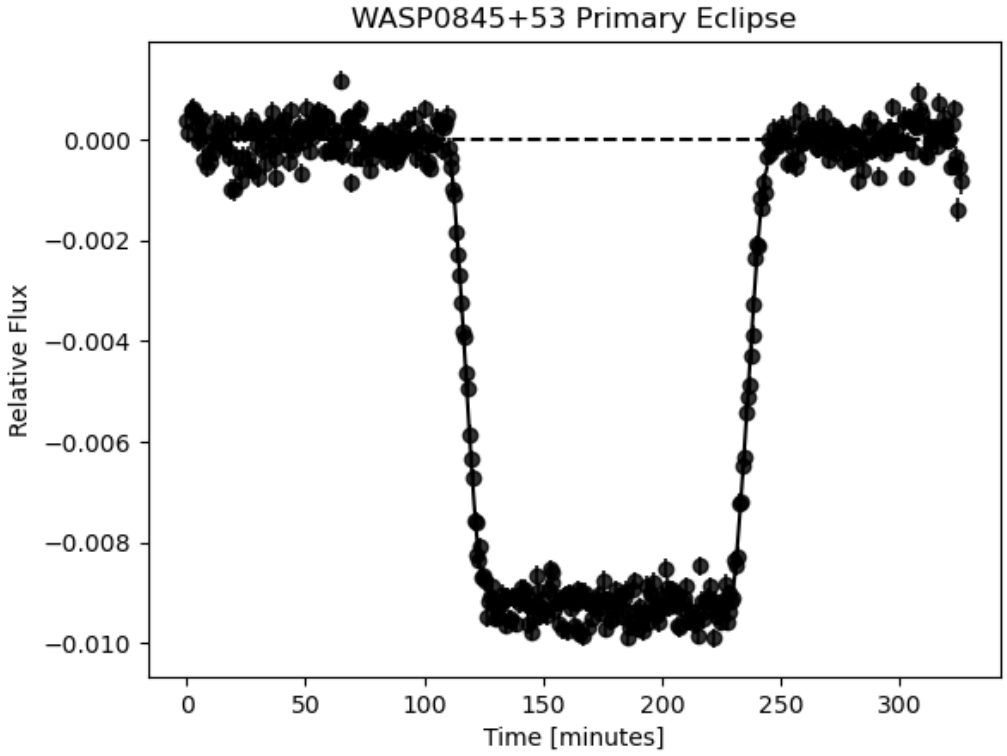

Figure 3. Light curve in R filter of primary eclipse after removal of systematic offset and piecewise polynomial fitting.

the primary. These timescales can be related to the orbital period of the binary system P via our constant velocity assumption:

$$\frac{2R_B}{\tau} = \frac{2R_A}{\tau + T} = \frac{2\pi a}{P} \tag{1}$$

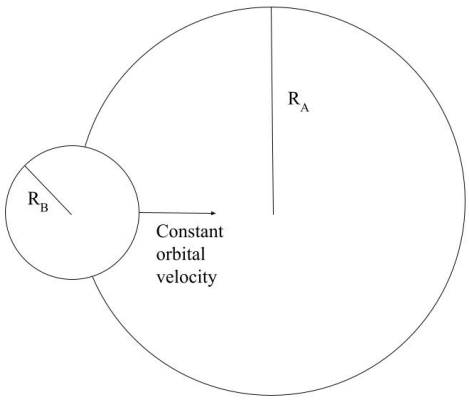

Figure 4. Diagram displaying the beginning of the primary eclipse as the pre-He-WD (radius R_B) transits in front of the primary star (radius R_A).

The variable a represents the semi-major axis, or orbital radius, of the system. Solving Equation 1 to find the orbital period in terms of R_A,

$$P = \frac{\pi(\tau + T)}{R_A/a} \tag{2}$$

By carefully eyeballing our light curve, we obtained $T = 0.072$ days and $\tau = 0.0105$ days after averaging the ingress and egress times. A more rigorous approach would be necessary to extract R_A/a and other parameters by fitting our light curve, however, this was beyond the scope of this project. Instead, we used the estimate of $R_A/a = 0.303 \pm 0.013$ from Maxted et al. to proceed with our analysis.

Using Equation 2, we estimated the orbital period to be

$$P = \frac{\pi(0.072 + 0.0105)}{0.303} = 0.855 \text{ days} \tag{3}$$

The ratio of R_B to R_A can also be solved for from Equation 1 in terms of just τ and T:

$$\frac{R_B}{R_A} = \frac{\tau}{\tau + T} = \frac{0.0105}{0.0105 + 0.072} = 0.127 \tag{4}$$

The result from Equation 4 can then be used to find the luminosity ratio of the secondary to the primary via:

$$\frac{L_B}{L_A} = (\frac{T_B}{T_A})^4 (\frac{R_B}{R_A})^2 \tag{5}$$

However, this requires estimates of the effective temperatures which we were not able to constrain in without rigorously fitting our light curve. Therefore, we again elect to use the estimates from Maxted et al. of $T_A = 8000 \pm 400$ K and $T_B = 15000 \pm 800$ K and find a luminosity ratio of

$$\frac{L_B}{L_A} = (\frac{15000}{8000})^4 (0.127)^2 = 0.2002 \tag{6}$$

5. DISCUSSION

Using the estimates given by Maxted et al. of $R_A/a = 0.303 \pm 0.013$ and $R_B/a = 0.0397 \pm 0.0028$, Maxted reports R_B/R_A to be approximately 0.131 ± 0.0108. Maxted also gives a orbital period of $P = 0.844 \pm 0.000003$ days. Our estimate of the orbital period is a slight overestimate but demonstrates that the system can be well approximated as a circular orbit. Our estimate of R_B/R_A falls within the 1σ uncertainty reported by Maxted. However, Maxted reports L_B/L_A as 0.0415 ± 0.0019, which is an order of magnitude lower than our estimate of 0.2002. This likely comes from the fact that effective temperatures given by Maxted are for a different filter and thus cannot be used for a one-to-one comparison of L_B/L_A.

To investigate the possibility of mass transfer between the stars, we explore the mass parameter space (M_B, M_A) over a range of masses typical for EL-CVn binaries to calculate a corresponding Roche lobe. An approximation for the Roche lobe r_b of a star of mass M_B is given by Eggleton (1983),

$$\frac{r_b}{a} = \frac{0.49q^{2/3}}{0.6q^{2/3} + \ln(1 + q^{1/3})} \tag{7}$$

where $q = M_B/M_A$. If $r_b < R_B$, mass transfer is likely occurring between the stars. In terms of the parameter space (M_B, M_A), this equation becomes

$$r_b(M_B, M_A) = \frac{0.49q^{2/3}}{0.6q^{2/3}a + \ln(1 + q^{1/3})} a(M_B, M_A) \tag{8}$$

where $a(M_B, M_A)$ comes from Kepler's Third Law:

$$a(M_B, M_A) = \left[\frac{(M_A + M_B)GP^2}{4\pi^2}\right]^{1/3} \tag{9}$$

We use the mass ranges reported by Chen et al. (2017) of $M_B = \{0.17, 0.21\}M_\odot$ and $M_A = \{1.3, 1.5\}M_\odot$ as a baseline for this parameter space and explore the regime slightly beyond these masses as well. Figure 5 visualizes the full mass parameter space, with contours to denote the corresponding Roche lobes. The boxed region contains the mass ranges given by Chen et al. For the masses estimated by Maxted et al., the corresponding Roche lobe is around $1R_\odot$. The typical radius of white dwarfs tends to be around 0.8-2% of $1R_\odot$ (Shipman 1979), therefore the radius of the pre-He-WD is likely too small to exceed the Roche lobe at the mass suggested by Maxted. The large gap between the current Roche lobe of the pre-He-WD and its expected radius could be evidence of significant mass transfer onto the primary star in the past, as this would explain how the pre-He-WD came to have such a low mass.

6. CONCLUSIONS

We report the following binary parameters of the EL-CVn system, WASP0845+53, in the R filter: $P = 0.855$ days, $R_B/R_A = 0.127$, and $L_B/L_A = 0.2002$. These parameters agree well with existing estimates given by Maxted et al. except for L_B/L_A, though we attribute this to the difference in bandpasses. The observed magnitude increase during a primary eclipse was found to be 0.0434. We leave it up to future to work to further constrain these parameters by utilizing a more rigorous approach to fitting our observed light curve.

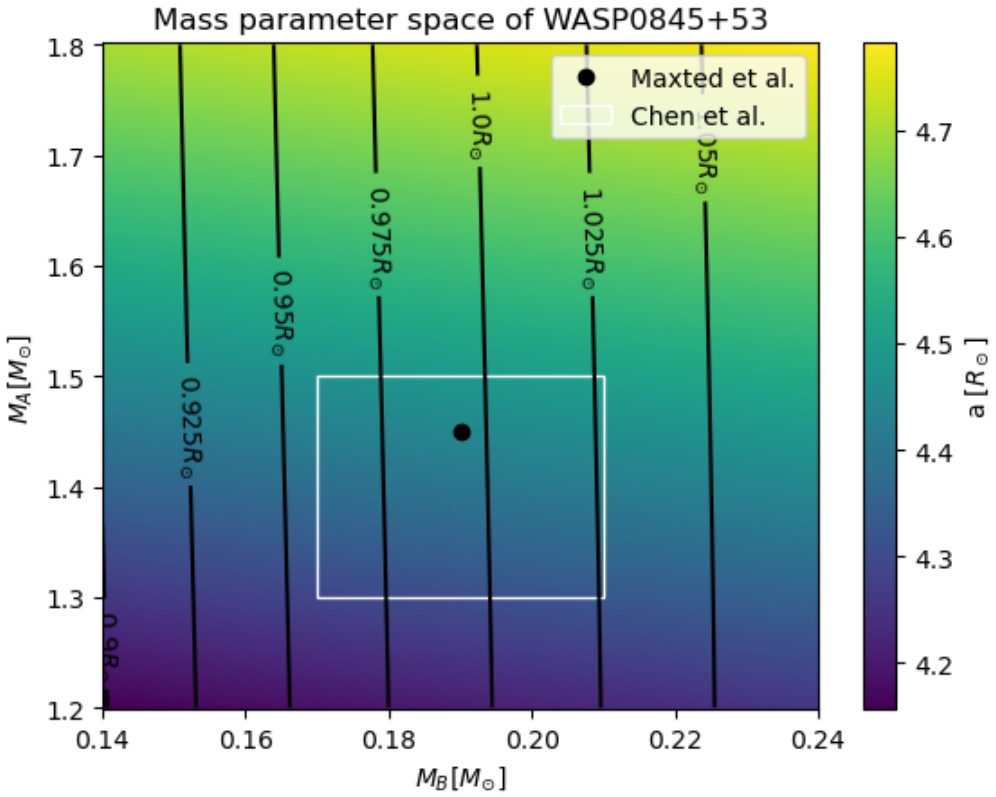

Figure 5. Mass parameter space of WASP0845+53. The black contours indicate corresponding Roche lobes while the colormap shows the corresponding orbital radii.

We conclude that mass transfer between the pre-He-WD and the primary star is not a valid description for the current state of this binary system, as the Roche lobe for the pre-He-WD far exceeds its expected radius. We propose that significant mass transfer from the secondary onto the primary star in the past provides the most viable mechanism for the current mass of the pre-He-WD, though other possible mechanisms for mass transfer such as stellar winds (Modisette & Kondo 1980) require more analysis to be ruled out. We hope that further multi-bandpass observations of WASP0845+53 can provide sufficient data to more precisely constrain the parameters of this EL-CVn binary.

7. ACKNOWLEDGEMENTS

We thank Dr. Bender and Dr. Green for all of their assistance with this project throughout the semester.

Facilities: 61" Kuiper Telescope (UofA)

Software: astropy (Astropy Collaboration et al. 2013, 2018), AstroImageJ (Collins et al. 2017)

REFERENCES

Astropy Collaboration, Robitaille, T. P., Tollerud, E. J., et al. 2013, A&A, 558, A33, doi: 10.1051/0004-6361/201322068

Astropy Collaboration, Price-Whelan, A. M., Sipőcz, B. M., et al. 2018, AJ, 156, 123, doi: 10.3847/1538-3881/aabc4f

Chen, X., Maxted, P. F. L., Li, J., & Han, Z. 2017, MNRAS, 467, 1874, doi: 10.1093/mnras/stx115

Collins, K. A., Kielkopf, J. F., Stassun, K. G., & Hessman, F. V. 2017, AJ, 153, 77, doi: 10.3847/1538-3881/153/2/77

Eggleton, P. P. 1983, ApJ, 268, 368, doi: 10.1086/160960

Maxted, P. F. L., Anderson, D. R., Burleigh, M. R., et al. 2011, MNRAS, 418, 1156, doi: 10.1111/j.1365-2966.2011.19567.x

Maxted, P. F. L., Bloemen, S., Heber, U., et al. 2014, MNRAS, 437, 1681, doi: 10.1093/mnras/stt2007

Modisette, J. L., & Kondo, Y. 1980, in Close Binary Stars: Observations and Interpretation, ed. M. J. Plavec, D. M. Popper, & R. K. Ulrich, Vol. 88, 123–126

Pollacco, D. L., Skillen, I., Collier Cameron, A., et al. 2006, PASP, 118, 1407, doi: 10.1086/508556

Shipman, H. L. 1979, ApJ, 228, 240, doi: 10.1086/156841